

Implicit subgrid-scale models in space–time variational-multiscale discretizations

S. J. Hulshoff^{*,†}

*Faculty of Aerospace Engineering, Delft University of Technology, Kluyverweg 1,
2629 HS Delft, The Netherlands*

SUMMARY

The behaviour of space–time variational-multiscale discretizations is investigated using a moving-wave solution of the one-dimensional viscous Burgers equation. Effects of spatial discretization parameters are demonstrated using time-converged numerical results. Two approaches for estimating implicit subgrid-scale energy dissipation are described, and the dependence of implicit dissipation on spatial discretization parameters is examined. Copyright © 2005 John Wiley & Sons, Ltd.

KEY WORDS: variational multiscale; space–time finite elements; large-eddy simulation

1. INTRODUCTION

Variational-multiscale (VMS) discretizations [1, 2] show promise for application to large-eddy simulations (LES) due to their consistency with the governing equations at large scales, and their consistent treatment of scale separation near boundaries. When combined with a finite-element method (FEM) [3], VMS discretizations can also be applied to complex domains. Time-discontinuous space–time FEM are particularly advantageous in this regard, as they naturally incorporate mesh movement, and allow arbitrary re-meshing from one time step to the next [6].

To account for the effects of unresolved scales, VMS methods normally employ a physical subgrid-scale (SGS) model. Like all discretization techniques, however, VMS discretizations introduce errors which are greatest in magnitude for the smallest resolved scales. These result in an implicit SGS model, which competes with the physical SGS model in the description of the effects of the unresolved scales. In FEM-based VMS discretizations, there are numerous parameters which influence the behaviour of the implicit SGS model. In order to gain insight into these influences, this paper examines the behaviour of the implicit SGS model for a

*Correspondence to: S. J. Hulshoff, Faculty of Aerospace Engineering, Delft University of Technology, 2600 AA Delft, The Netherlands.

†E-mail: S.J.Hulshoff@LR.TUDELft.NL

*Received 27 April 2004
Revised 28 September 2004
Accepted 5 October 2004*

space–time VMS-FEM discretization of the Burgers equation. Although it is widely known that the Burgers energy cascade relies on different mechanisms than those present in the Navier–Stokes cascade, it remains useful for the testing of LES algorithms due to its clear interpretation.

The most common approach to analysing implicit SGS models is based on the derivation of the modified equation using Taylor-series approximations (see Reference [4] for an example). This approach is not directly applicable to time-discontinuous space–time discretizations, however, for two reasons. Firstly, the derivation of modified equations for time-discontinuous discretizations requires the solution of a system of non-linear equations, which inhibits interpretation in terms of physical models. Secondly, the use of the higher-order interpolations inherent in the VMS-FEM approach, combined with the non-smooth nature of LES problems, means that one is not necessarily in a range where examination of only the leading terms of the Taylor series is justified. Therefore in this paper, results from a series of numerical simulations are used to examine the effects of discretization parameters on the implicit SGS model. To simplify interpretation, a test case which allows accurate estimation of the parameters of the physical SGS model is employed.

In order to illustrate the general influence of spatial discretization parameters, results with negligible time-discretization errors are first considered. Results from two methods for estimating the strength of the implicit SGS model are then discussed, and the behaviour of the implicit SGS model is examined for realistic time steps.

2. DISCRETIZATION

For a space-continuous, time-discontinuous Galerkin discretization on a space-periodic domain, the viscous Burgers equation may be represented as

$$\begin{aligned}
 B(w, u) &= (w, u_t + uu_x - vu_{xx} - f)_Q = 0 & (1) \\
 &= -(w_t, u)_Q - \left(w_x, \frac{u^2}{2} - vu_x \right)_Q - (w, f)_Q \\
 &\quad + (w, u^-)_{\Omega^{n+1}} - (w, u^+)_{\Omega^n} + (w, (u^+ - u^-))_{\Omega^n} & (2)
 \end{aligned}$$

Here $(\cdot, \cdot)_Q$ represents the L_2 inner product on the space–time domain, while $(\cdot, \cdot)_{\Omega^n}$ and $(\cdot, \cdot)_{\Omega^{n+1}}$ are the L_2 inner products on the boundary of the domain at times $t = t^n$ and $t = t^{n+1}$. The solution is advanced in time by solving a sequence of space–time domains with thickness $\Delta t = t^{n+1} - t^n$ (slabs), with the Ω^{n+1} boundary of each slab providing the initial condition for the following slabs. The initial condition is imposed weakly, using the last term in (2) (see Reference [6] for details).

The discretization is implemented as a VMS method by employing a hierarchical basis, and interpreting its components in terms of large and small scales. Here, the hierarchical basis consists of the standard bilinear functions supplemented with r Legendre polynomials in space. These polynomials are defined to be zero at the nodes. The solution interpolation

within an element is then

$$u(x, t) = \sum_{i=1}^n N_i(x, t) a_i + \sum_{j=1}^r \beta_j(x, t) b_j \tag{3}$$

where n are the element nodes, $N_i(x, t)$ are the bilinear ‘tent’ functions, and β_j are products of Legendre polynomials in space with a linear basis in time. The interpolation is continuous in space, so that nodal a_i values are shared between elements.

The discrete solution, u , and the test function w are assumed to lie in the function space \mathcal{V} . Following References [1, 3], \mathcal{V} is partitioned so that $\mathcal{V} = \bar{\mathcal{V}} + \mathcal{V}'$, $u = \bar{u} + u'$, and $w = \bar{w} + w'$, where $\bar{\cdot}$ and \cdot' denote the large and small resolved scales. From the argument of scale separation, it is assumed that the direct interactions between the unresolved scales and the large resolved scales are negligible. In contrast, the effects of the unresolved scales on the small resolved scales are represented by an additional physical SGS model, M . The large- and small-scale equations are then

$$B(\bar{w}, \bar{u}) = -B(\bar{w}, u') + (\bar{w}_x, (\bar{u}u'))_Q \tag{4}$$

$$B(w', u') = -B(w', \bar{u}) + (w'_x, (\bar{u}u'))_Q + M \tag{5}$$

where \bar{u} is associated with the linear and low-order Legendre components of (3), and u' is associated with the high-order Legendre components. For the following study a Smagorinsky-like physical SGS model is employed, $M = -(w'_x, \nu_T u'_x)_Q$, with the turbulent viscosity coefficient ν_T defined to reproduce the dissipation of the unresolved scales.

3. BURGER’S TEST CASE

The test case is defined by (1) with $\nu = 2\pi/1000$ and $f(x, t) = A \sin(x - Ut)$, where $U = 1$, $A = 0.1$. This produces a moving wave with the large-time profile shown in Figure 1(a). DNS computations of this problem were performed on a sequence of meshes to ensure grid independence. The finest of these used 8192 bilinear space-continuous elements on a domain of length 2π , with a constant time step of $\pi/8192$. The computations were started with a uniform flow of $U = 1$, and advanced to $t = 8\pi$. After $t = 6\pi$, the solution profile remains essentially constant. The final fine-mesh energy spectrum, along with the spectra of two very coarse computations, is shown in Figure 1(b). The constant solution profile of this test case is advantageous, in that it allows the parameters of the physical SGS model to be accurately estimated. In particular, given the wave number range to which the physical SGS model will be applied, the finest DNS solution is used to estimate ν_T with

$$\nu_T = \nu \frac{\int_{k_c}^{\infty} k^2 E(k) dk}{\int_{k_m}^{k_c} k^2 E(k) dk} \tag{6}$$

where $E = u^2/2$ is the kinetic energy, k_m is the starting wave number of the physical SGS model range, k_c is the cut-off wave number, and the spectral definition of the energy dissipation rate has been used (see Reference [5]). For VMS-FEM, the cut-off wave number is defined

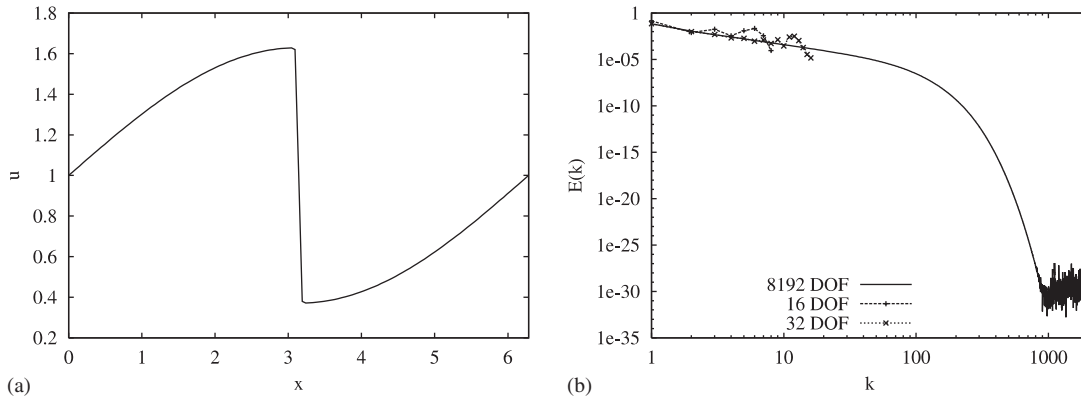


Figure 1. (a) DNS solution and (b) energy spectra.

by $k_c = qN/2$, where N is the number of elements, and q is the number of unique unknowns per element along a constant-time boundary. This is equal to the number of spatial modes which can be represented by the discretization, although for higher values of q , these discrete modes are not spatially harmonic. The first spatial interpolation function to which the physical SGS model is applied is denoted by m . The gradients for the model are computed using all scales above and including m , and the model is applied to all scales above and including m . k_m is estimated by multiplying the ratio of scales without modelling to the total number of scales by k_c .

The procedure described above minimizes the calibration error of the physical SGS model, so that differences in the results can be clearly related to the choice of discretization parameters. An alternative approach to minimizing the effects of the physical SGS model is to set $M=0$, which forces all energy dissipation to be accounted for by the implicit SGS model. This is undesirable in that it results in the unrealistic large- k energy pile-ups shown in Figure 1(b).

4. COMPUTED RESULTS

4.1. Spatial discretization effects at small time steps

The behaviour of the discretization at a time step equal to that of the finest DNS is considered first. Figure 2 shows the error in the time average of the total kinetic energy relative to the DNS between $t=6\pi$ and 8π . This interval is equal to the period necessary for the wave to completely traverse the mesh. The errors are plotted *versus* the inverse of the number of degrees of freedom used to represent the solution in space, which varies from 16 to 128. The solid line labelled 'Basic LES' indicates the results obtained for $q=1, m=1$.

The errors of the $q=2$ and $q=3$ solutions were found to be almost identical to those for $q=1$, when M is applied to all scales. Releasing the first scale from the physical SGS model ($q=2, m=2$), however, results in a large increase in accuracy. The latter implies that the errors of the basic LES cases are dominated by the application of the physical SGS

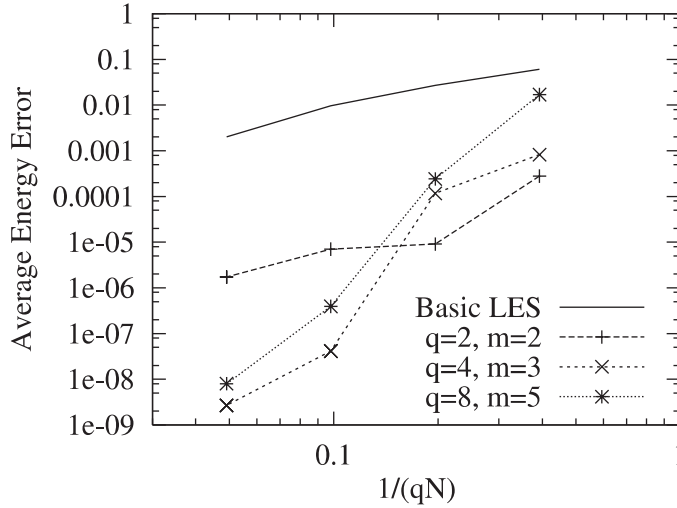


Figure 2. Average energy error for different numbers of scales.

model to the largest resolved scales, rather than by specifics of the discretization. A significant advantage of the VMS approach is that it limits the distortion of the large scales by shifting the application of the physical SGS model to the smaller resolved scales. The latter is consistent with the idea that the unresolved scales interact strongly with the smallest of the resolved scales, and only indirectly with the largest resolved scales.

Increasing the order of the method while keeping k_m/k_c constant ($q=4, m=3$ and $q=8, m=5$) results ultimately in a faster convergence rate, but larger errors at low numbers of degrees of freedom. The corresponding errors in the solution profile have high spatial frequencies, and arise from the non-smooth solution of the LES problem.

4.2. Implicit SGS model

In the stationary solution of the test problem, there is a balance between the work done by the body force, and the energy dissipated by viscosity and the implicit SGS model. One method for estimating the implicit SGS dissipation is thus to subtract the resolved change in energy due to viscosity per time step from the work done by the body force per time step, ΔE_f :

$$\Delta E_{\text{ISGS}} = \Delta E_f - \sum_e^N \int_{Q_e} (v(u_x)^2 + v_T(u'_x)^2) dQ_e \tag{7}$$

where Q_e is the space-time domain of element e . An alternative approach is to estimate the change in the energy of the linearized system with $v=v_T=0$ for identical discretization parameters. In Figure 3(a) the normalized implicit dissipation, $E_{\text{ISGS}}/\Delta E_f$ computed with (7) for $q=2, m=2$ is compared with the estimate from the $v=v_T=0$ linearized system for varying values of the Courant number, $U\Delta t/\Delta x$. In spite of the relatively large perturbation to the mean convection speed, the estimates agree reasonably well. For the current problem parameters, both estimates approach the theoretical third-order convergence rate of the time discretization [6].

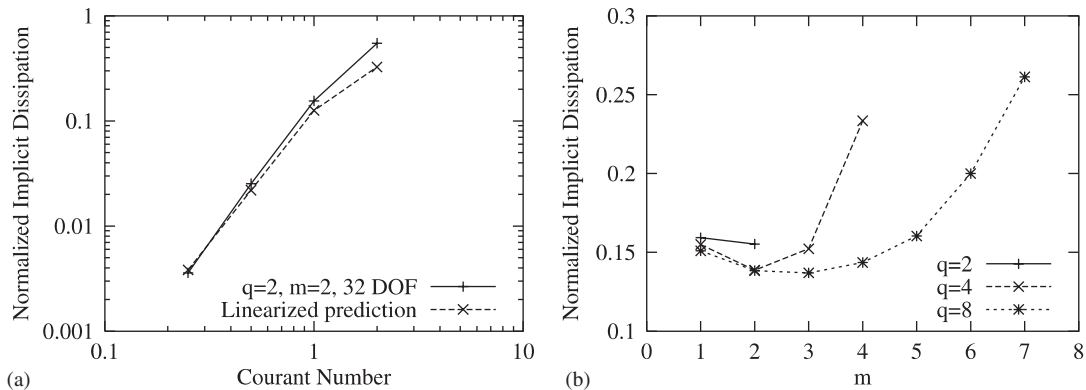


Figure 3. Normalized implicit SGS energy dissipation.

The influence of spatial discretization parameters on the implicit SGS model is shown in Figure 3(b). Here, the normalized implicit dissipation based on (7) is plotted for different values of q and m for $qN = 32$ and a Courant number of 1. Independent of q , there is an initial drop in the implicit dissipation as m is increased from 1. When larger numbers of scales are released from the model, however, the implicit dissipation begins to increase. Fourier analysis of the linearized system for low-order discretizations indicates that the primary action of the implicit SGS model is to damp high-frequency components of the solution [6]. As m is increased, M is applied to a higher range of frequencies with larger values of ν_T . This biases the energy towards low frequencies, where the implicit model is less active. For the largest values of m , however, the increase in spatial order results in strong high-frequency errors, and correspondingly increased implicit dissipation. The action of the implicit SGS model is thus minimized at intermediate values of m .

5. CONCLUSIONS

Using a one-dimensional test case, this paper has demonstrated effects of discretization parameters on the performance of a space-time VMS FEM, and on its associated implicit SGS model. The VMS method was shown to be advantageous, in that it can improve the accuracy of large-scale data by limiting the application of the physical SGS model to the smaller resolved scales. There is a limit to the number of scales which can be released from the model, however, due to the lack of smoothness of the underlying solution.

The magnitude of the implicit SGS dissipation was primarily influenced by the time step, but was also shown to be influenced by the number of model-free scales. Again low numbers of free scales per element proved best, as larger numbers resulted in increased implicit dissipation associated with the high-frequency errors of higher-order discretizations. For a moderate ratio of free scales, however, the choice of the total number of scales per element was not found to significantly affect the implicit dissipation at a fixed number of degrees of freedom.

REFERENCES

1. Hughes TJR, Mazzei L, Jansen KE. Large eddy simulation and the variational multiscale method. *Computation and Visual Science* 2000; **3**:47–59.
2. Hughes TJR, Oberai AA, Mazzei L. Large eddy simulation of turbulent channel flows by the variational multiscale method. *Physics of Fluids* 2001; **13**(6):1784–1799.
3. Collis SS. The DG/VMS method for unified turbulence simulation. *AIAA Paper No. 2002-3124*, 2002.
4. Margolin LG, Rider WJ. A rationale for implicit turbulence modeling. *International Journal for Numerical Methods in Fluids* 2002; **39**:821–841.
5. Saffman PG. Lectures on homogeneous turbulence. In *Topics in Nonlinear Physics*, Zabusky NJ (ed.). Springer: Berlin, 1968.
6. Shakib F, Hughes TJR. A new finite element formulation for computational fluid dynamics: IX. Fourier analysis of space-time Galerkin/least-squares algorithms. *Computer Methods in Applied Mechanics Engineering* 1991; **87**:35–58.